Chem Soc Rev

From 1 → 3 Dendritic Designs to Fractal Supramacromolecular Constructs: Understanding the Pathway to the Sierpiński Gasket

Journal:	*Chemical Society Reviews*
Manuscript ID:	CS-REV-07-2014-000234.R1
Article Type:	Review Article
Date Submitted by the Author:	09-Jul-2014
Complete List of Authors:	Newkome, George; Dean of the Graduate School, Office of the Vice President for Research Moorefield, Charles

Journal Name

RSCPublishing

ARTICLE

From 1 → 3 Dendritic Designs to Fractal Supramacromolecular Constructs: Understanding the Pathway to the Sierpiński Gasket

Cite this: DOI: 10.1039/x0xx00000x

Received 00th January 2012,
Accepted 00th January 2012

DOI: 10.1039/x0xx00000x

www.rsc.org/

George R. Newkome*[a,b] and Charles N. Moorefield[b]

The iterative synthetic protocols used for dendrimer construction were developed based on the desire to easily craft highly branched macromolecules with ideally an exact mass and tailored functionality. Inspired by arboreal design and precursors of the utilitarian macromolecules known as dendrimers today, our first examples employed predesigned, 1 → 3 or 1 → (1+2) *C*-branched, building blocks. Physical characteristics of the dendrimers, including their globular shapes, excellent solubility, and demonstrated aggregation, revealed the inherent supramolecular potential. The architecture that is characteristic of dendritic materials also exhibits obvious *fractal* qualities based on self-similar, repetitive, branched frameworks. Thus, both the fractal design and supramolecular aspects of these constructs are suggestive of a larger field of fractal materials that incorporate repeating geometries and are derived by complementary building block recognition and assembly. Use of <terpyridine-M^{2+}-terpyridine> connectivity for the sides and tuned directed organic vertices has opened the door to other types of novel materials. This approach also circumvents the nonideality of dendrimers, since the heteroleptic, one-step, spontaneous self-assembly process facilitates quantitative outcomes.

In the 1970s, a television program created and presented by James Burke called "Connections" interwove historical events that were proposed to support the creation of novel inventions or devices. Burke spun together a series of theoretical inter-relationships that supported his premises. Of course, Hercule Poirot, Sherlock Holmes, Monk, Jack Reacher, and most detectives do the same thing to solve a fictional mystery. What connections can be made that explain how new chemical innovations occur? How does one go from inspiration from mathematics or the natural world to new chemical molecules?

In the pre-computer chemical age, one went to the library, generally starting with Beilstein and spent hours looking up historical data in the myriad of journals written in diverse languages – oh yes, you needed a working knowledge of at least German and French besides English. But as one searched the literature, paging through the volumes of chemical transformations, it was impossible not to notice the structures, formulae, on all of those other pages in-between the research that one was searching for. And thus, as new monthly issues arrived in the science library or as one received one's own personal copies (journals were fairly inexpensive at that time) it was standard practice to read what was going on in other fields. So a morning a week, most researchers scanned for the latest, and in my case, synthetic gems. This was a treasure trove of odd-ball facts and observations that would shape our imaginations and became the stimulus for where our synthetic futures would go.

It is obvious that the "old" days are over, since now most scientific literature is electronically stored and managed thus making it, for the time being, rather difficult to scan or peek at the adjacent articles for those interesting but as yet unrelated structural inspirations. It is also very interesting that today few scientific articles are cited dating before 1985 because most are/were not cross-referenced for easy accessibility. Thus, many things are now being re-discovered and re-reported "for the first time".

This introduction gives the preamble to how structural relationships between Mother Nature, mathematics and our synthetic endeavors started. I

scanned a fascinating article entitled "Tree Architecture" written by Professor Tomlinson, director of the Harvard Forest, in *American Scientist*[1] in which he pictorially showed the architectural patterns of the trees in the rain forests of South American. How could anyone catalogue those rain forests into 18 architectural designs? But there they were! Then my new knowledge of the Leeuwenberg model (Figure 1) permitted me to mentally replace each of the tree's branching point with a sp^3 C atom. Branching 1 → 3 became, and still is, a very efficient route to arborols and dendritic materials.

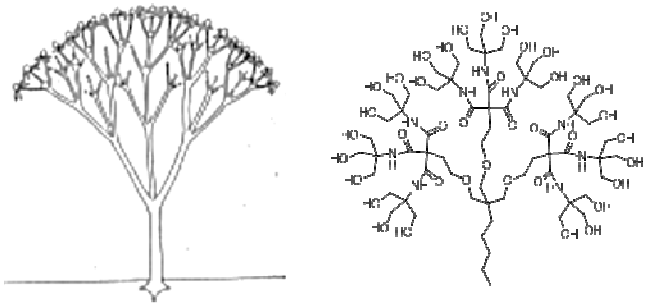

Figure 1. Leeuwenberg's tree model[1] *vs.* the 27-arborol[3] [Reproduced by permission of *American Scientist*, magazine of Sigma Xi, The Scientific Research Society, P. B. Tomlinson, *Am. Sci.* 1983**, 71**, 141 and The American Chemical Society, Newkome, *et al., J. Org. Chem.*, 1985, **50**, 2003].

In today's lexicon, this is a perfect example of biomimicry ("bio" = life and "mimic" = copy) in which Mother Nature's designs show us how biological entities have evolved over the millennia.[2] Poorer designs were lost and the best ones survived and offer more efficient adaption to their environment. In 1983, it was that mental connection of two different topics – the architecture of a tree and an sp^3 carbon atom[3] – but, today biomimicry is intellectually stimulating the construction of many structural similarities, which have led to the design of gecko tape, the Japan's shinkansen bullet train, wind turbines, and entropy carpet, to note but a few.

Dendrimers have further been demonstrated to be examples of molecular fractals[4-7] based on their repeating architectural motif at differing size scales and directly associated with biomimicry.[8] It is the fractal quality of the dendrimer that has given rise to new types of materials.

Notably, dendrimers are but a small component within the world of fractals. Molecular architectures exhibit self-similarity on differing scales to allow incorporation of a balance of interrelated attributes and structural components that are ideally suited for interdependent component positioning. Towards these directions, we have been designing, testing, and assembling nanoscale homo- and heteronuclear materials possessing a non-branched morphology in which metal center incorporation and structural architecture join with supramolecular concepts to facilitate material applications. The use of ligand-metal-ligand connectivity has thus served to expand our directed and self-assembly work into the novel, utilitarian "*fractal*" macro- and nano-molecular, architectural arena.[9]

In 2006, we reported the first chemical synthesis of a nondendritic fractal construct[9] (Figure 2), based on the Sierpiński hexagonal gasket, which incorporates both the Star of David as well as a Kock snowflake designs. This was assembled in a three-step process *via* the adaptation of the facile self-assembly of substituted *meta*(*bis*terpyridinyl)benzene in the presence of one equivalent of Fe^{2+} affording a high yield of the desired metallomacromolecular hexagon.[10] Key questions that we asked at the time were: can one synthesize such fractal constructs in one-step and can assemblies approach quantitative yields?

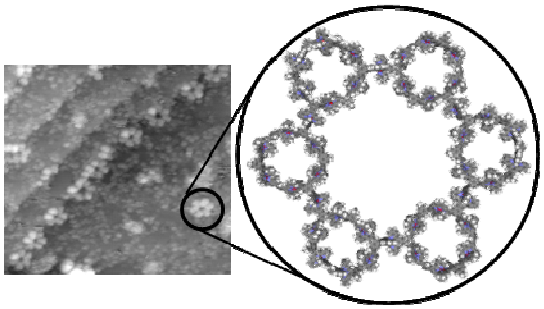

Figure 2. Space-filling depiction of the first synthetic organic Sierpiński hexagonal gasket and its STM image[9] [Reproduced with permission from AAAS, G. R. Newkome, *et al.*, *Science*, 2006, **312**, 1782].

As witnessed over the past half century, chaos science has introduced us to a methodology that permits insight into the observed order and patterns that were noted earlier as one dissects the designs that are imbedded in the complexity within Nature. Thus, the elements of chaos, fractals, and dynamics have been introduced to mathematically address that complexity. To actually demonstrate the close structural relationship between 1 → 3 branched dendrimers and Sierpiński fractals, specifically the Sierpiński triangle can be readily envisioned in Figure 3. This unique structural relationship was introduced in "Chaos and Fractals. New Frontiers of Science" by Peitgen and his

colleagues.[11,12] In their marvellous compendium, they introduced a figure that superimposed a 3-directional, 2D branched fractal onto a specific triangle, which Sierpiński mathematically envisioned nearly a century ago.[13] The dendritic branches bisect the collective triangle sides' at all midway points demonstrating the structural relationship between dendrimers and another fractal nonbranched pattern (Figure 2).

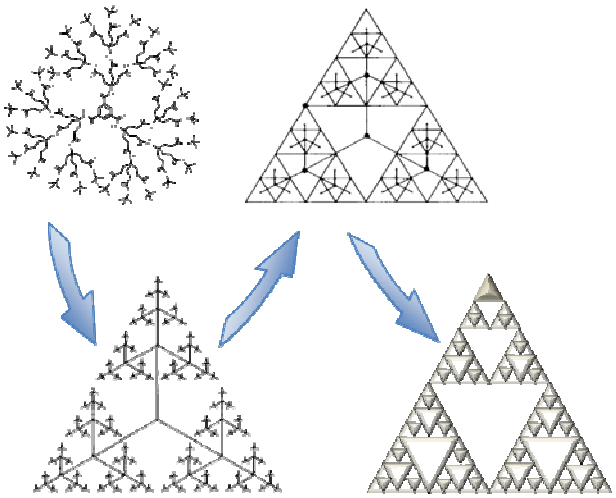

Figure 3. The Serpiński triangle and its geometrical relationship to a 1 → 3 *C*-branched, dendrimer.[11]

The use of ligand-metal-ligand connectivity, specifically substituted terpyridine coupled with different divalent metals, was the starting point for this task. Thus, the vertices would be the tailored organic components that would possess the proper directivity to instill the eventual shape of the polygon. The side of the polygon would use terpyridine-M^{II}-terpyridine (<tpy-M^{II}-tpy>) connectivity. The metals can be tailored for molecular stability or easy structural reversibility. The specific utilitarian properties can thus be readily incorporated, based on the desired oxidized and reduced metal states; thus leading to novel molecular devices,[15] such as in new photovoltaic cells and organic light emitting diodes (OLEDs),[14] based on their photo- and electroluminescence properties,[15] and as well as molecular switches[16] and optical display components,[17] founded on their low/high spin characteristics. These attributes coupled with the potential to self-assemble the fractal materials into nanotube and nanofiber structures make them ideal candidates for bio-pharma applications. This tutorial is intended to give a brief overview of the key structural issues as well as introduce the reader to the molecular world *via* traditional mathematics and the beauty of Mother Nature's fractal patterns.

Building block architectures are dependent on the physical and chemical properties of the desired material under construction; although at times, the properties of the new materials are not readily apparent based solely on the building block(s) design. This leads to an evolution in materials' synthesis and utility, as well as an element of excitement and anticipation with regard to the discovery of unknown local and aggregate attributes. This expansion into other fractal patterns should follow a similar paradigm to those of the tree-like dendrimers.[18-20]

From the first published reports in the mid-1980s, dendrimers and dendritic materials, characterized by a regularly repeating, branched motif that may be simply described as tree-like, have captured the attention of research groups around the globe. This is due in-part to several factors, including the potential to integrate the dendritic constructs with other materials in order to instill the desired physical or structural properties generating the tailored molecular assembly possessing the enhanced physical and/or structural characteristics for a utilitarian outcome. For example, high molecular weight species can easily be made soluble in aqueous or non-aqueous media, based on the incorporated surface functionality. As well, and perhaps more importantly, with the advent of dendritic synthetic strategies, chemists now have better insight to incorporate precise structural control over the placement of the desired components of macromolecular materials that can be fully and unequivocally characterized.

Notably, dendrimer construction has been conceived and developed in many variations. Building from the outside inward complements the reverse construction from the inside outward (convergent *vs.* divergent protocols). Dendron attachment has been effected using a wide variety of covalent and non-covalent protocols. As well, dendrimers can be constructed using linear building blocks, where branching centers are created during generational growth. Dendrimers have been examined in a numerous applications, including chemical[21,22] and electrical sensing,[23] micellar host-guest ability,[24] coatings and polymer additives,[25] and drug delivery vehicles.[26-34]

The past several years have witnessed increased interest in the general topic of metallodendrimers, particularly in relation to their future nanotechnological applications.[32,35-37] Thus, projected research directions should build on the melding of classical synthetic strategies with materials science protocols to fine-tune bulk and localized supramolecular properties to specific tasks and to assemble macromolecular infrastructures

capable of functioning alone or in concert within materials at composite interfaces.

The art of macromolecular construction has evolved to include utilitarian composite materials; whereby, interdependent components are precisely matched for the desired physicochemical properties. Targeted materials and properties, derived from minimum-assembly protocols, are therefore of interest from various perspectives that include the ease of architecturally complex construction and commercial viability. The preparation of new monomers with bonding metal center(s) leading to new predesigned macro- and nano-scale constructs includes: branching multiplicity and choice of branching moieties (*e.g.* mono- or polyatomic), length and flexibility of connector units, coupled with localized and aggregate supramolecular properties. Thus, fundamental supra-macromolecular properties can be affected by subtle changes in these design parameters.

The single-step, high yield, self-assembly of a hexaruthenium macrocycle (**2**, Scheme 1) possessing the ubiquitous benzenoid architecture derived from the 120° juxtaposed ditopic ligand, 3,5-*bis*(terpyridinyl)-

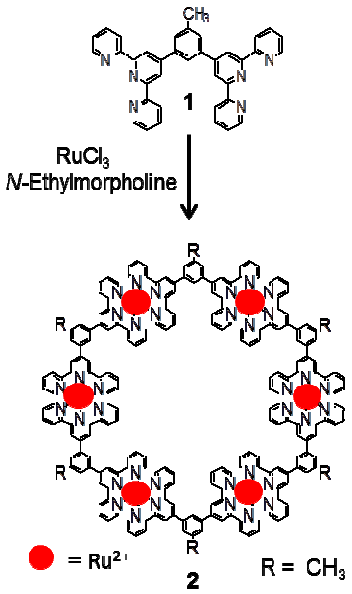

Scheme 1. Self-assembly of a rigid hexameric metallo-macrocycle **2**[38] [Reproduced with permission from Wiley-VCH, G. R. Newkome, *et al*., *Angew. Chem. Int. Ed.*, 1999, **38**, 3717].

toluene (**1**) was realized.[38] The resultant metallo-macrocycle supports a 12^+ charge and was isolated as the Cl^- salt; ion exchange to the PF_6^- salt facilitated characterization and solubility in common organic solvents. Structural confirmation of this original hexameric, multimetal array was supported by TEM imaging. These multimetal arrays readily aggregate into larger assemblies, which presented opportunities to easily generate new ion-promoted, stoichiometric self-assembly of nanoscale composite fibers (Scheme 2). Thus, combining this structurally rigid hexameric macrocycle $[(\mathbf{2}^{12+})(PF_6^-)_{12}]$ with a flexible, dodeca-carboxylate-terminated, first generation, 1 → 3 branched dendrimer[39] $[(\mathbf{3}^{12-})(Na^+)_{12}$ gave rise to rigid fibers[40] $[(\mathbf{2}^{12+})(\mathbf{3}^{12-})]_n$, as revealed by TEM images (Figure 4).

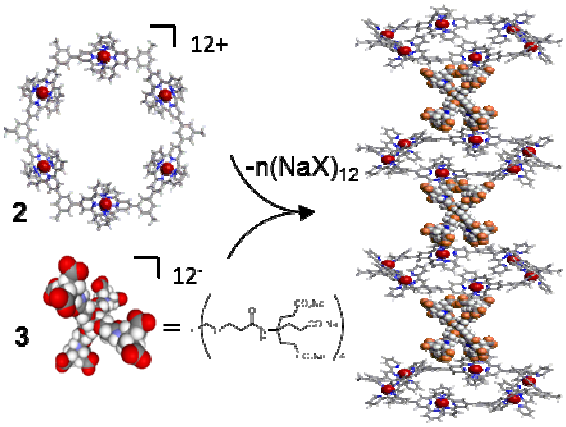

Scheme 2. Assembly of a metallomacrocycle-dendrimer nanocomposite[40] [Redrawn with permission from Wiley-VCH, P. Wang, *et al*., *Adv. Mater*. 2008, **20**, 1381].

The hydrodynamic diameter for the dendrimer of 23.6 Å determined under basic pH conditions using 2D diffusion ordered spectroscopy (DOSY) NMR experiments[41] is larger than the internal open area diameter (17.5 Å) of the hexamer. This suggests that an ordered, molecular packing of the two components could be based on the dendrimer fitting above (and below) the cavity of the hexamer, and only partially into it. Insight into the composites molecular ordering was

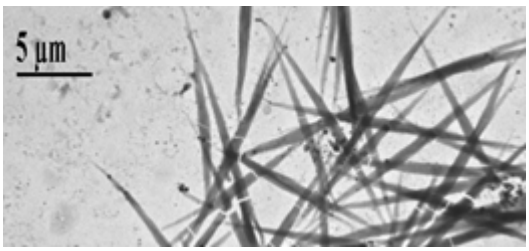

Figure 4. Rigid fibers[40] $[(\mathbf{2}^{12+})(\mathbf{3}^{12-})]_n$ [Reproduced with permission from Wiley-VCH, P. Wang, *et al*., *Adv. Mater*. 2008, **20**, 1381].

obtained with selected area electron diffraction (SAED) of these fibers. Two strong electron diffractions perpendicular to the fibers long axis were observed with a *d*-spacing of 3.85 nm; diffused higher diffractions were also observed. As well, a *d*-spacing of 1.92 nm was obtained from a pair of intense diffraction patterns parallel to the fiber's long axis. This suggests that the in-plane direction of ($\mathbf{2}^{12+}$) is perpendicular to the long axis and that self-assembly results in alternating stacking of the two components.

These fractal constructs have led to the development of materials with demonstrated potential as: molecular batteries, switches, and optical display devices, to name but a few (Figure 5).[42-46] Hence, these research directions necessarily encompass studies on <tpy-M^{II}-tpy> connectivity employing preconstructed synthons in order to facilitate the desired one-step construction (as opposed to the multi-step construction of dendrimers) of nano- and macroscopic, precisely positioned, polymetal arrays giving rise to designer multicomponent macromolecular systems.

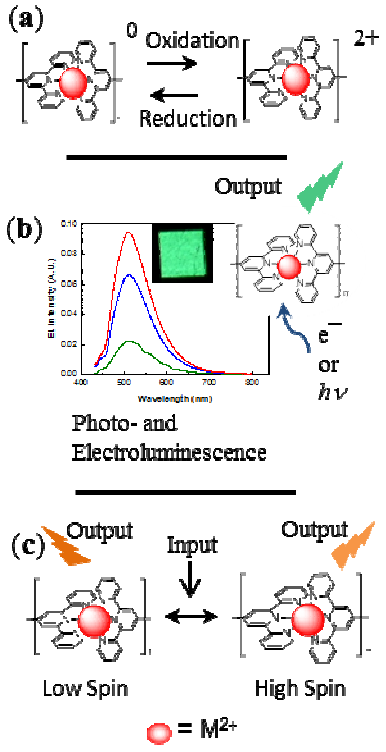

Figure 5. Potential uses for metallomacrocycles (a) energy storage, (b) optical devices, and (c) molecular switches.

With the impetus to explore the properties of triangular metallocycles,[47,48] three new ligands (**4**; Scheme 3) possessing 60° directionality were prepared by a Suzuki coupling[49] with known dihaloarenes with 4-terpyridinylphenylboronic acid.[50] Treatment of these 60°-based *bis*terpyridines with either Cd^{2+} or Zn^{2+} generated a series of triangular materials (**5**) that were observed to form fibers, following counterion exchange with benzenehexacarboxylate. These linear, hair-like

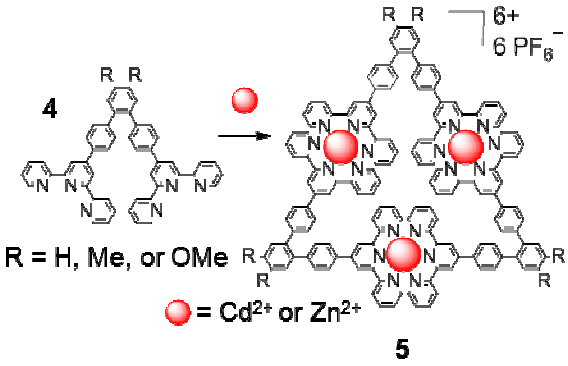

Scheme 3. Preparation of triangular metallocycles[51] [Redrawn with permission from The Royal Society of Chemistry, A. Schultz, *et al*., *Dalton Trans.* 2012**, 41**, 11573].

fibers[51] were obtained using a mixed solvent system prepared from dilute solutions (~1 mM) of metallocycle in MeCN and sodium hexabenzoate in water. TEM images (Figure 6) revealed large bundled structures with cross-sections of *ca.* 300 nm comprised of narrower

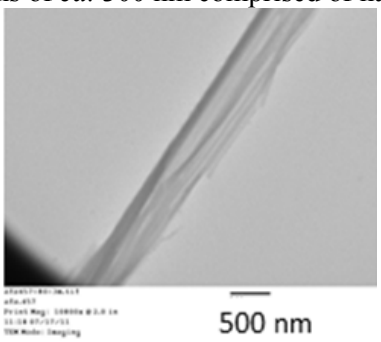

Figure 6. TEM image of the fibers derived from **5** with sodium hexabenzoate[51] [Reproduced with permission from The Royal Society of Chemistry, A. Schultz, *et al*., *Dalton Trans.* 2012**, 41**, 11573].

fibrous strands of *ca*. 2 nm. Rigorous characterization of these molecular triangles included electrospray ionization mass spectrometry (ESI-MS) in concert with traveling-wave ion mobility mass spectrometry (TWIM-MS), along with gradient tandem mass spectrometry (gMS^2) that corroborated the stability of the triangles observed in the TWIM spectra. Powder X-ray diffraction (XRD) data were obtained from microcrystalline regions within the fibers. Combined

with SAXD data orthorhombic unit cell dimensions of 39.82, 8.38, and 49.14 Å for a, b, and c, respectively, were determined and a packing model (Figure 7) for the triangles in the fiber was suggested using computer generated molecular modelling.

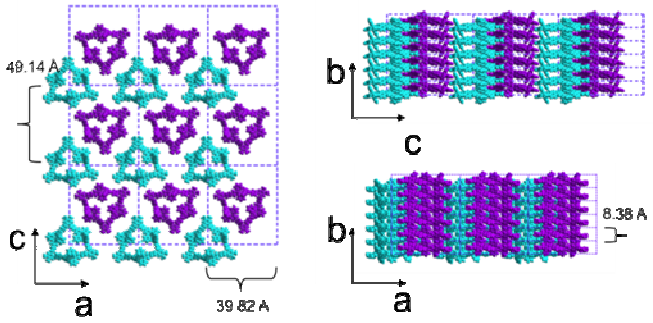

Figure 7. Proposed fiber packing model for triangle **5** and sodium hexabenzoate[51] [Reproduced with permission from The Royal Society of Chemistry, A. Schultz, *et al*., *Dalton Trans.* 2012**, 41**, 11573.]

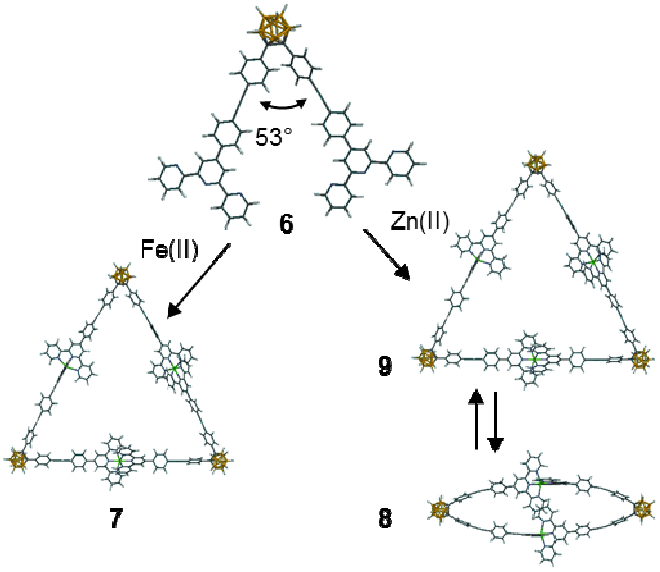

Figure 8. With the right metal monomer **6** assembles to give the Zn^{2+} triangle **9** and dimer **8**[53] [Redrawn with permission from The Royal Society of Chemistry, J. Ludlow, *et al*., *Dalton Trans.*, 2014**, 43**, 9604].

The self-assembly of the related 1,2-*bis*[4'-(4-ethynylphenyl)-2,2':6',2"-terpyridinyl]-*o*-carborane (**6**) using either Zn^{2+} or Fe^{2+} in a precise 1:1 ratio gave, not the reported polymer,[52] but rather a series of small macrocycles (**7**) in which with Fe^{2+} the main product was the triangle.[53] However with Zn^{2+} under thermodynamic control, the NMR data revealed a dynamic equilibrium between the entropically favored dimer (**8**) and the enthalpically favored trimer (**9**) (Figure 8).[54] Kurth *et al.* have, however, shown[55] that the simple, linear ditopic ligand 1,4-(*bis*[2,2':6',2"]-terpyridine-4'-yl)benzene with Fe^{2+} can generate giant, self-contained metallosupramacromolecular rings with a diameter of 73 nm of which each layer contains *ca.* 7600 metal ions and ligands. Whereas, this linear ligand with Fe^{2+} readily self-assembles in the presence of dihexadecyl phosphate (DHP) to generate a polyelectrolyte-amphiphile complex,[56] which forms a Langmuir film possessing a stratified architecture with the DHP forming a monolayer on the water surface while the metallosupramacromolecular coordination polyelectrolyte is immersed in the aqueous subphase.

Self-assembly techniques generally lead to the most thermodynamically stable product(s), while kinetic control is required to access those that are less stable. For example, kinetic control can be affected by utilizing non-reversible connectivity to achieve the desired target or by the removal of the potential for the formation of

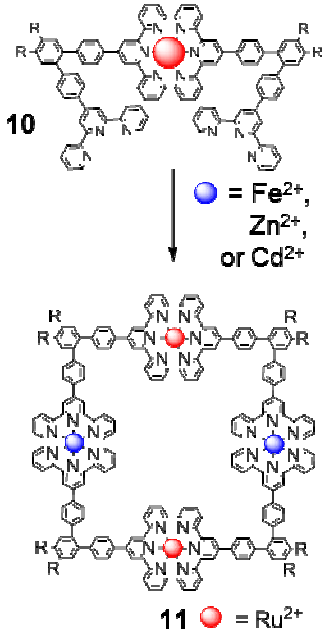

Scheme 4. Synthesis of square-shaped metallocycles **11** from the distorted dimer **10**[57] [Redrawn with permission from Wiley-VCH, A. Schultz, *et al*., *Chem. Eur. J.* 2012**, 18**, 11569].

the enthalpically favored product. Since, the high yield synthesis of trimeric metallocycles by the self-assembly of 60°-based *bis*terpyridines has been demonstrated, the dimerization of these *bis*ligands using strongly binding metals that can render the complex non-reversible leading to the formation of folded molecular squares upon self-assembly with itself.[57] With ligand **4** (Scheme

4), dimerization was achieved by a stoichiometrically controlled reaction with $RuCl_2(DMSO)_4$[58] in $CHCl_3$: MeOH (1:1 v/v) to generate the highly directed *bis*ligand **10**. Self-assembly with Ru^{2+}, Fe^{2+}, Zn^{2+}, and Cd^{2+} gave the corresponding tetramers **11**, respectively. For the Cd^{2+} and Zn^{2+} products, purification was achieved by simple counterion exchange with NH_4PF_6; whereas, the Fe^{2+} and Ru^{2+} tetramers required column chromatography. Notably, a one-pot reaction of ligand **4** with $FeCl_2{\cdot}4H_2O$ afforded (8%) a Fe^{2+} tetramer (not shown), along with the expected trimer in 29% yield, after chromatography. In addition to NMR, ESI-MS, TWIM-MS, and photophysical characterization, gradient tandem MS (gMS^2) revealed an order of stability for stability order of <tpy-M^{II}-tpy> as Cd^{2+} < Zn^{2+} < Fe^{2+} < Ru^{2+}, as expected. Owing to the unique folded shape of these tetramers (Figure 9), the descriptive term "Dondorff" rings was coined after the first person to describe the giant manta ray.

Figure 9. Computer generated model of a tetrameric Dondorff ring **11** possessing the folded shape[57] [Reproduced with permission from Wiley-VCH, A. Schultz, *et al*., *Chem. Eur. J.* 2012**, 18**, 11569].

In an earlier report, the concept of utilizing larger, dimeric, *bis*terpyridine ligands to afford a series of heteronuclear hexameric, octameric, and decameric metallocycles[59] *via* stepwise self-assembly procedures has been reported. In this case, the new *bis*ligand **12** was constructed using a 120°-based building block (**1**) architecture (Scheme 5). As in the case of the 60°-juxtaposed starting ligand, the formation of smaller metallocycles is circumvented when a longer building block is used as the precursor.

Traveling wave ion mobility mass spectrometry (TWIM-MS) and molecular modeling provided insight into their unique sizes and conformational flexibility. Dimer **12** was isolated (29%) from a single-pot reaction of the corresponding 120°-based *bis*(terpyridine) ligand with 0.5 equivalent of $RuCl_2(DMSO)_4$.[58] Treatment of **12** with 1.05 equivalents of $FeCl_2{\cdot}4H_2O$ in MeOH afforded the ditopic hexamer **13**, octamer **14**, and decamer **15** in 36, 9, and 2% yields, respectively, after column chromatography. The specific geometries of the different macrocycles and their cross-sectional areas were investigated using molecular modeling and annealing simulations. Their collision cross-section *vs.* relative energy plots exhibited three distinct areas, corresponding to three major regions of conformations: circular, twist stretched, and twist folded. Whereas, when rigid ligands are used to construct the macrocycles, the overall flexibility of the larger polycomplexes increases with size, leading to a wider range of possible geometries. Flexibility is thus greatest for decamer **15** (Figure 10), where several different conformers are possible.

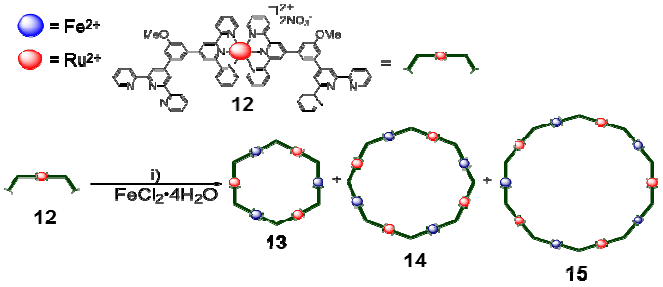

Scheme 5. Construction of heteronuclear larger metallomacrocycles.[59] [Redrawn with permission from Wiley-VCH, Y.-T. Chan, *et al*., *Chem. Eur. J.* 2011**, 17**, 7750.]

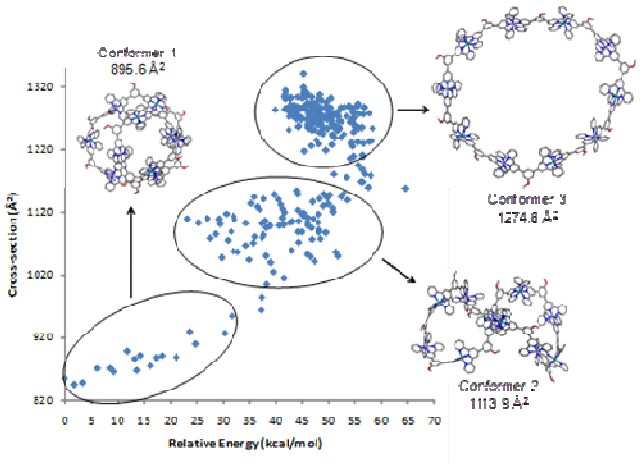

Figure 10. A plot of collision cross-sections *vs*. relative energies for **15**.[59] [Reproduced with permission from Wiley-VCH, Y.-T. Chan, *et al*., *Chem. Eur. J.* 2011**, 17**, 7750.]

Expanding on the concept of enlarging *bis*ligand building blocks for the construction of otherwise not easily accessible macrocycles, a trimeric ligand **17** has been designed, prepared, and isolated.[60] Following a two-step reaction sequence, whereby *bis*terpyridine **16** was treated with 2 equivalents of $RuCl_3$ to give the

paramagnetic *bis*Ru^{3+} adduct, which upon addition of 2 equivalents of **16** under reductive conditions afforded the desired trimer **17** (Scheme 6).

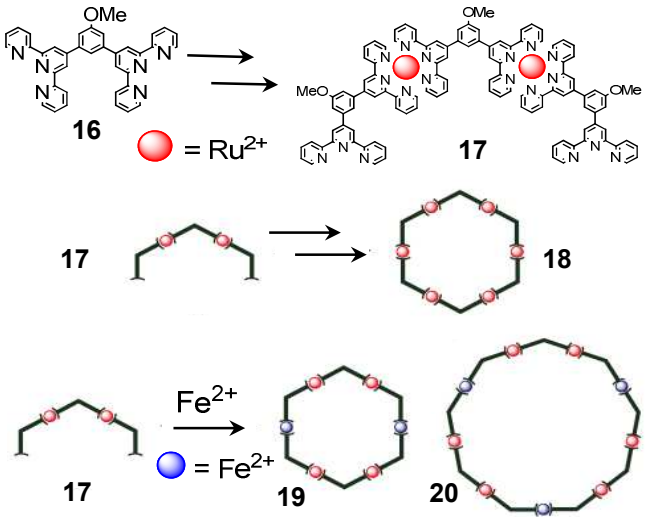

Scheme 6. Synthesis of trimer **17** and its conversion into homo- and hetero-nuclear metallomacrocycles[60] [Reproduced with permission by The American Chemical Society, Y.-T. Chan *et al*., *J. Am. Chem. Soc.*, 2011**, 133**, 11967].

Incorporating *bis*terpyridine **17** into the same two-step sequence gave (80%) the desired hexaRu^{2+} metallocycle **18**. Reaction of trimer **17** with $FeCl_2$ in refluxing MeOH for 18h generated the heteronuclear hexamer **19** and nonamer **20** in 49 and 14% yields, respectively. Their characterization by ESI-TWIM-MS, ^1H and ^{13}C NMR, absorption spectroscopy, molecular modelling, and 2D DOSY (diffusion ordered spectroscopy) supported the similar ring sizes of the two hexamers, as well as the larger nonamer; diffusion coefficients of 4.57×10^{-10}, 4.51×10^{-10}, and 3.31×10^{-10} m^2/s were recorded for the homo- and hetero-nuclear hexamers and heteronuclear nonamer, respectively.

Efforts aimed at the construction of pentameric metallomacrocycles have utilized carbazole derivatives to introduce the requisite angle.[61] Thus, employing a 3,6-disubstituted carbazole unit between two ligands gave a 105° angle between two directed terpyridine ligands (*i.e.* **21**). Treatment of the carbazole-based *bis*terpyridine **21** with Ru^{2+}, Fe^{2+} or Zn^{2+} gave the corresponding metallocycles **22**, (Scheme 7). Employed as sensitizer materials for solar cell devices, discharge experiments were conducted to support this utilitarian application. A similar fill factor (*ff*) was observed for the three electrodes studied, while both the short circuit photocurrent (j_{sc}) and the open circuit photopotential (V_{oc}) exhibited the best results for the Ru^{2+} metallopentacycle. As well, photoconversion efficiency (η) using light covering the visible region of the spectrum again showed that the Ru^{2+} pentamer possessed the highest value.

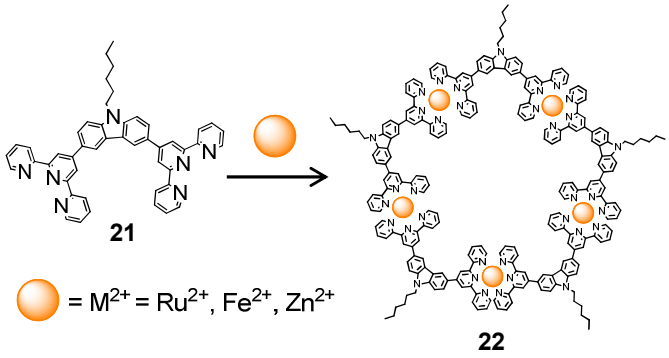

Scheme 7. Synthesis of pentameric metallocycles **22** possessing carbazole subunits[61] [Reproduced with permission from The Royal Society of Chemistry, S.-H. Hwang, *et al*., *Chem. Commun.* 2005, 4672].

After modifying a 120°-based *bis*terpyridine ligand with an acetyl protected sugar moiety, the expectation of crafting a peripherally functionalized, hexameric metallomacrocycle was realized (12% isolated yield) along with the unexpected uniquely constrained, pentameric construct (4%).[62] Thus, the Fe^{2+}-based pentamer **23** - characterized unequivocally by 2D COSY NMR and ESI-MS - represents the first example of a smaller ring being obtained from the self-assembly of rigid, 120°-juxtaposed terpyridine ligands. A noticeable difference in the ^1H NMR of **23** in contrast to the related hexamer was the upfield shift of the absorption attributed to the 4Ar*H*, that is oriented towards the interior of the ring; a slightly enhanced crowding effect for the five-membered specie was postulated. All other NMR absorptions for both rings were very similar. Both the five- (**23**) and six-membered rings formed fibers when hexane was allowed to diffuse into a solution of the macrocycle in a $CHCl_3$:MeOH:MeCN mixture (8:3:1 v/v). In each case, fiber lengths and diameters of 10-80 nm and 20-30 nm were observed, respectively (Figure 11). Molecular modelling of the rings showed interior void regions of 1.3 nm for the 5-membered specie and 1.8 nm for the larger ring.

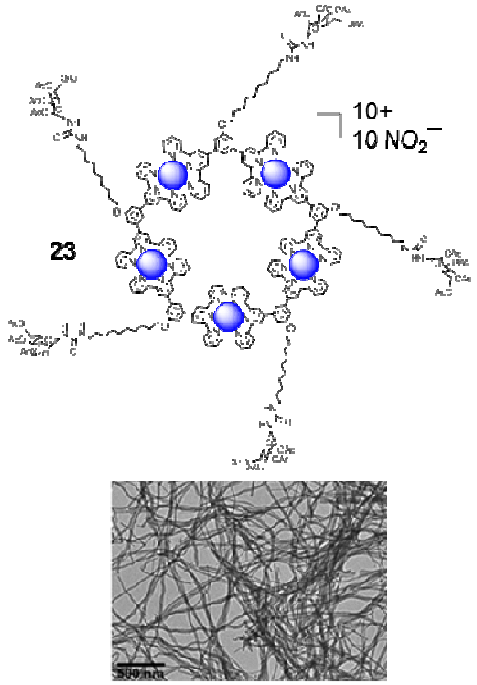

Figure 11. The sugar coated pentamer **23** self-assembled to generate needle-like fibers[62] [Reproduced with permission from Wiley-VCH, Y.-T. Chan *et al*., *Chem. Eur. J.* 2010**, 16**, 1768].

After starting to comprehend the issue of controlling ring size, a better understanding of thermodynamic control over the self-assembly of the metallomacrocycles was necessary to address the issue(s) associated with a predictable quantitative self-assembly, *i.e*. use of Cd^{2+} to facilitate <tpy-Cd^{II}-tpy> connectivity to provide the kinetic *vs*. thermodynamic balance. Thus, treatment of *tert*-butyl-modified *bis*terpyridine **24** with a stoichiometric amount of $Cd(NO_3)_2 \cdot 4H_2O$ in $CHCl_3$:MeOH (3:2 v/v) quantitatively generated the desired hexacadmium macrocycle **25** (Scheme 8).[63] Due to the labial issues associated with the <tpy-Cd^{II}-tpy> coordination, the thermodynamically most stabile hexameric product was formed; no other linear or cyclic species were detected. Ions selected for ion mobility separation included $[6L+6Cd]^{4+}$ and $[3L+3Cd]^{2+}$, based on the small number of ligand-to-metal possible combinations. Ion mobility separation signals for the cyclic and linear fragments generated from the cyclic material occurred at shorter drift times (*i.e*., 10.30, 6.45, and 5.13 ms for the $[3L+3Cd]^{2+}$ ion and linear and cyclic $[6L+6Cd]^{4+}$ ions,

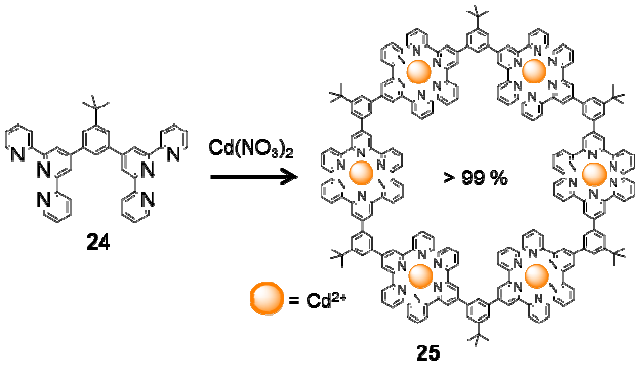

Scheme 8. Quantitative construction of the Cd-based hexamer **25**[63] [Reproduced with permission from The American Chemical Society, Y.-T. Chan, *et al*., *J. Am. Chem. Soc.* 2009, **131**, 16395].

respectively) then the signals for same *m/z* 1187 amu-based fragments observed in the case of the linear construct (*i.e*., 11.55 and 6.59 ms for linear $[3L+3Cd]^{2+}$ and the $[6L+6Cd]^{4+}$ ions respectively). Drift times are longer for the linear building block material and no signals were seen near the lower drift time of 5.13 ms, which confirmed that the 5.13 peak corresponds to the cyclic $[6L+6Cd]^{4+}$ species and the 6.45 ms peak corresponds to the linear $[6L+6Cd]^{4+}$ species. Thus, the linear fragments generated from the cyclic material in the mass spectroscopy instrument arise solely from the cyclic specie.

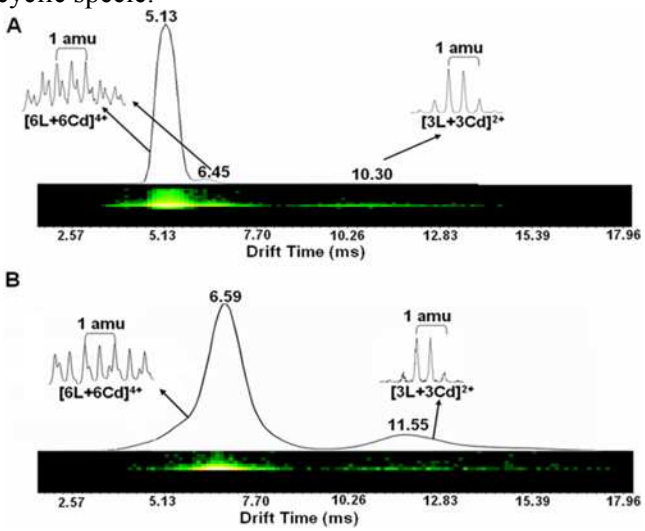

Figure 12. The 2D ESI-TWIM-MS signals[63] (**25**) for the m/z 1187 amu (A) compared to the same ion fragments generated from a similar linear Cd construct (B) [Reproduced with permission from The American Chemical Society, Y.-T. Chan, *et al*., *J. Am. Chem. Soc.* 2009, **131**, 16395].

The ability to create new materials with terpyridine-based self-assembly processes is limited only by the building blocks that are available and the imagination of the chemist. Ready availability of two additional tetrabromoarenes synthons facilitated the creation, *via* the high yield Suzuki coupling reaction, of two isomeric tetra*kis*terpyridines [*i.e.*, **26** (80 %) and **27** (40 %), Scheme 9]. With these new isomers added to our molecular arsenal, two polycyclic, macromolecular, constitutional isomers were easily constructed by application established procedures.[64] As in the case of synthesizing large ring structures, use of the dimeric terpyridine **10** restricted the degrees-of-freedom of reaction and subsequently facilitated optimum conditions for isolation of either molecular bowtie **28** (80%) when reacted with tetra*kis*terpyridine **26** or the isomeric molecular butterfly motif **29** (75%) when treated with tetra*kis*terpyridine **27**. Of particular interest are the notably different drift times observed in the ion mobility separation mass spectra that unequivocally demonstrated the different sizes and morphologies of these isomers at high charge states.

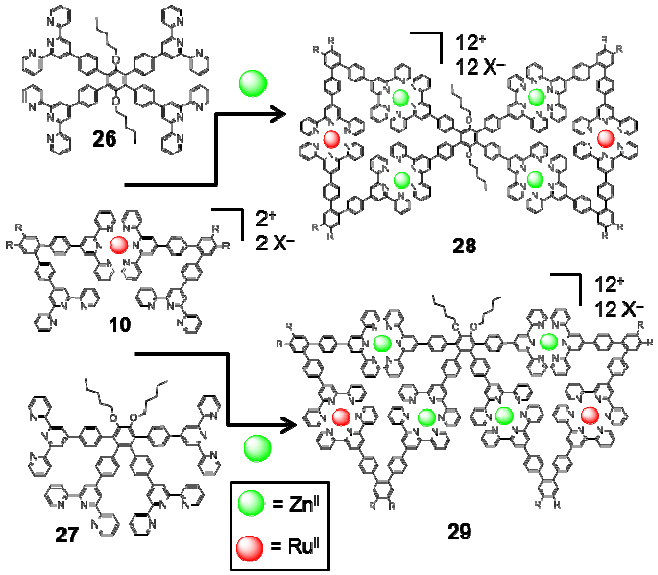

Scheme 9. Self-assembly of isomeric bowtie (**28**) or butterfly (**29**) bicyclic metallomacrocycles[64] [Redrawn with permission from The American Chemical Society, A. Schultz *et al*., *J. Am. Chem. Soc.* 2012**, 134**, 7672.].

In an effort to examine the outcome(s) of reacting building blocks with differing geometries,[48] two new *bis*terpyridine "V"-type ligands **30** and **31** (120°- and 60°-oriented, respectively) were constructed. Reaction of these two building blocks with $Zn(NO_3)_2{\cdot}6H_2O$ in a precise 2:1:1 ratio in MeOH for 30 min at 25 °C afforded the rhomboidal complex **32** (Scheme 10). Analysis by ESI-MS revealed the presence of the simpler triangular species **32**, which can also be prepared in high yields by simply reacting building block **31** with a divalent metal. Performing the reaction under refluxing conditions for 24 h gave the same mixture. And, replacing $Zn(NO_3)_2{\cdot}6H_2O$ with $Cd(NO_3)_2{\cdot}4H_2O$ gave Cd^{2+}-based product mixtures of rhombus and triangle, as revealed by ESI-MS.

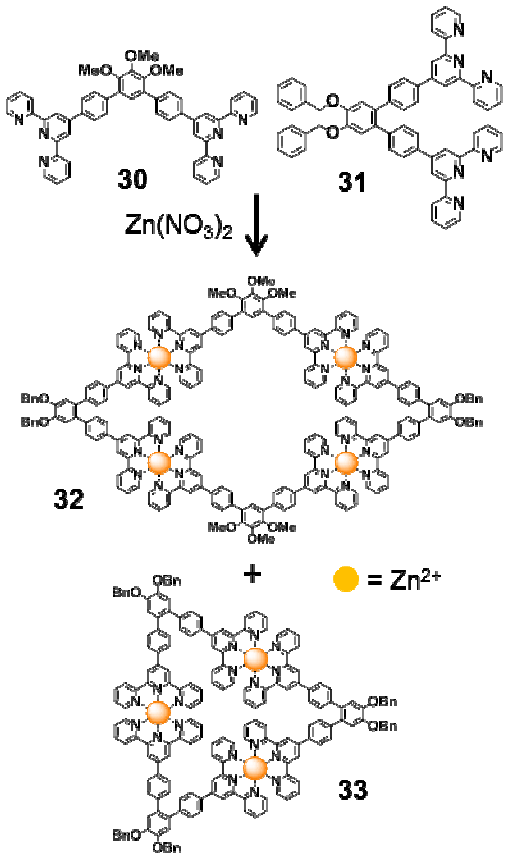

Scheme 10. Initial attempts to prepare a simple rhomboidal macrocycle[48] [Redrawn with permission from The Royal Society of Chemistry, X. Lu, *et al*., *Chem. Commun*. 2012, **48**, 9873].

To further probe the self-assembly a rhomboidal structures, *tris*terpyridine **34** was prepared (a "W" ligand); notably, it is a structural hybrid possessing both the 60°- and 120°-based ligands. Upon treatment of monomers **31**and **34** and $Zn(NO_3)_2{\cdot}6H_2O$ in a ratio of 2:2:5 in MeOH at 25 °C for 30 min, followed by ion exchange with NH_4PF_6, a slightly yellow fused *bis*-triangle (*i.e.*, rhombus **35**) was obtained in >95% yield without further purification (Scheme 11).[43] Unequivocal characterization was obtained with 2D COSY and NOESY NMR, along with ESI-TWIM-MS, which

showed the complete absence of the simple triangle-based by-product (**33**). It is also worth noting that the Zn-complex of **35** possesses remarkable stability in that it was observed to remain intact when subjected to MALDI-ToF-MS analysis in the linear mode. Normally, only Ru-based constructs have survived these conditions. In a logical extension of the polyterpyridines used in the construction of this rhomboidal structure, other polybromides were sought that would allow access to unique starting materials that will lead to fused triangular materials.

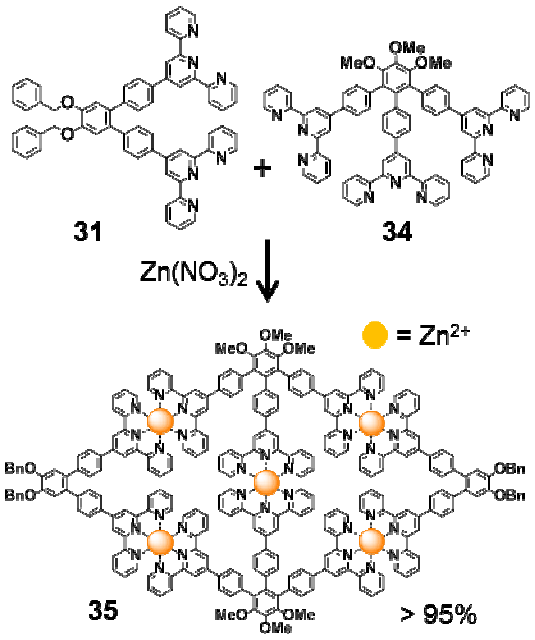

Scheme 11. Quantitative construction of a bridged rhomboid **35**[48] [Redrawn with permission from The Royal Society of Chemistry, X. Lu, *et al*., *Chem. Commun.* 2012, **48**, 9873].

In a dramatic example of the synthetic potential that complementary geometric and thermodynamic control can achieve, the first *bis*terpyridine-based, nanoscale, two-dimensional, supramolecular spoke wheel was constructed based on the formation of six adjacent triangles. *Tris*terpyridine **34**[65] and the known hexa*kis*terpyridine **36**[66] (Scheme 12) were each prepared using Suzuki-type, cross-coupling reactions with 4-terpyridinylphenylboronic acid and the corresponding tri- or hexabromobenzene. A three-component, single-step, coordination-driven, self-assembly with *tris*- (**34**) and hexa*kis*terpyridine **36** along with either Zn^{2+} or Cd^{2+} ions in a $CHCl_3$/MeOH solution at 25 °C for <30 min in a stoichiometric 6:1:12 ratio, respectively, generated the desired D_{6h} symmetric wheel **37** in >94% yield.[65] (Scheme 12) Characterization of the product included TWIM-MS, diverse NMR techniques, and TEM imaging. The polynitrate form was converted to the 24 PF_6^- salt to facilitate characterization. The TEM (Figure 13) supported the size and geometry of individual macromolecules revealing hexagonal-shaped, shadow-like images possessing average diameters of 6.5 ± 1.0 nm; this diameter corresponds well with the molecular modelling calculations showing a 5.6 nm diameter for the optimized structure.

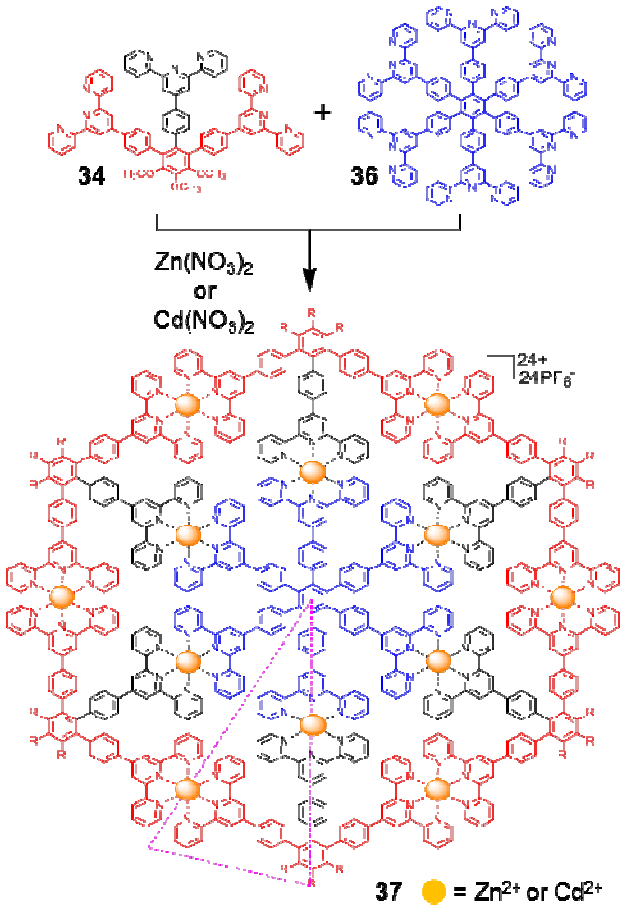

Scheme 12. Self-assembly of the D_{6h} symmetric, spoked wheel. Note the dotted triangle which represents the smallest repeating subunit[650] [Reproduced with permission from The American Chemical Society, J.-L. Wang, *et al.,* 2011**, 133**, 11450].

Two different approaches to a three-dimensional spoke wheel were devised in order to understand the importance of directional rigidity and to be able to quantitatively tailor the resultant shape; thus, the above 2D wheel's backbone and connectivity components were redesigned. The new 3D framework was derived from molecularly distorted building blocks: the core **36** was replaced with two equivalents of the *tris*terpyridinyl

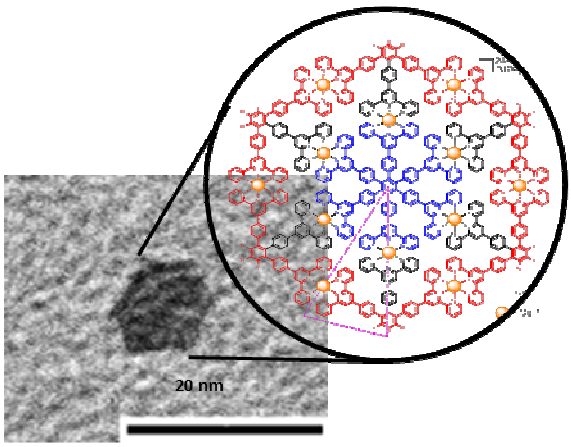

Figure 13. The TEM of the macromolecular wheel **37**[65] [Reproduced with permission from The American Chemical Society, J.-L. Wang, *et al.,* 2011**, 133**, 11450].

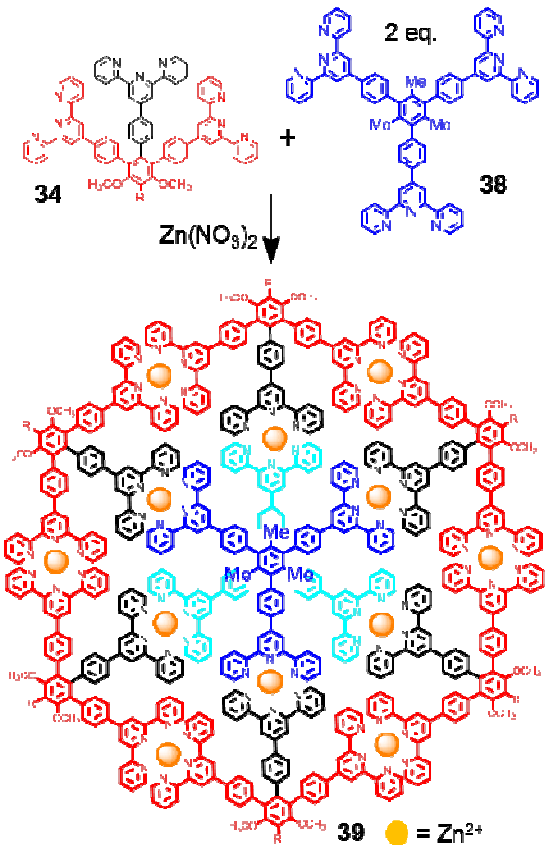

Scheme 13. Synthesis of the 3D, symmetric spoked wheel **39**.[67] The core terpyridines are shown as shades of blue [Redrawn with permission from Wiley-VCH, X. Lu, *et al.*, *Angew. Chem. Int. Ed.*, 2013**, 52**, 7728].

ligand **38**. The inherent molecular distortion incorporated into this rigid ligand is ideal for the spontaneous self-assembly in the presence of metal^{2+} and also possesses a methoxy marker for analysis of the resultant product. Therefore, 2 equivalents of **38** and 6 equivalents of **34** with precisely 12 equivalents of Zn^{2+} gave a single product that is the desired 3D wheel **39** (Scheme 13).[67] In each of these cases, it is critical that the components are soluble in the initial solvent mixture and to ascertain the singularity of these highly symmetric products based on the NMR of the product. As the structure becomes larger, the problems noted in our original Serpiński hexamer,[9] which possessed no discernable labels to help ascertain the presence of molecular symmetry - thus low temperature STM was needed to ascertain the hexameric infrastructure.

In order to ascertain the role of inherent molecular distortion in the construction modules, it was noted that two equivalents of the rim "W" component could also be used to generate a *bis*-rhomboidal-shaped core that would be ideally aligned with the rim components. Thus, the distortion within hexasubstituted ligand **34** could be organized so that it can play a dual role of core and rim. Thus, 8 equivalents of "W" ligand **34** along with 12 equivalents of Zn^{2+} gave (91%) a single product, which was shown to be the novel 3D, *bis*-rhomboidal shaped molecular wheel **40** (Scheme 14).[68] Although its single component composition was easily ascertained *via* MS, this molecularly skewed wheel possessed limited symmetry; thus, the overall structure even with the imbedded markers was based on very careful analysis of 2D COSY and NOESY NMR data and then the incorporation of a central aryl ring (OMe-OBn-OMe), so that the chemical shift data could be utilized to ascertain its internal location. This type of self-assembly utilizing highly distorted arenes possessing directed tripyridine moieties offers an interesting high yield avenue to complex rigid 3D nanoconstructs.

These above molecular wheels were quantitatively generated in one-step, in minutes, from multicomponents and thus these examples start to open a new synthetic door to the nanoscale world. Recently, Murata *et al.*[69] used DNA tiles and DNA origami to construct crystals containing a cellular automaton pattern. They initially chose the Sierpiński triangle design, since it requires only a small set of tiles as well as it would utilize all of the major assembly mechanisms in which errors could occur. Their work points out that one can control the thermodynamics and kinetics of multistage self-assembly processes in a simple one-pot series of reactions. Recently, Nieckarz and Szabelski have reported[70] a useful theoretical study into directing the self-assembly in metal-organic adsorbed adlayers in which the relative populations of

different conformers of rod-like organic building blocks, which can form directed coordination bonds, were controlled. They then set their sights on the simulated construction of the Sierpiński triangle by using linear prochiral organic linkers and three-coordinate metal centers.[71] In this case, they utilized metals at the vertices and linear organic connecters, which has been the major synthetic combination used by most chemists to create a vast array of specific self-assembled constructs.[72-75]

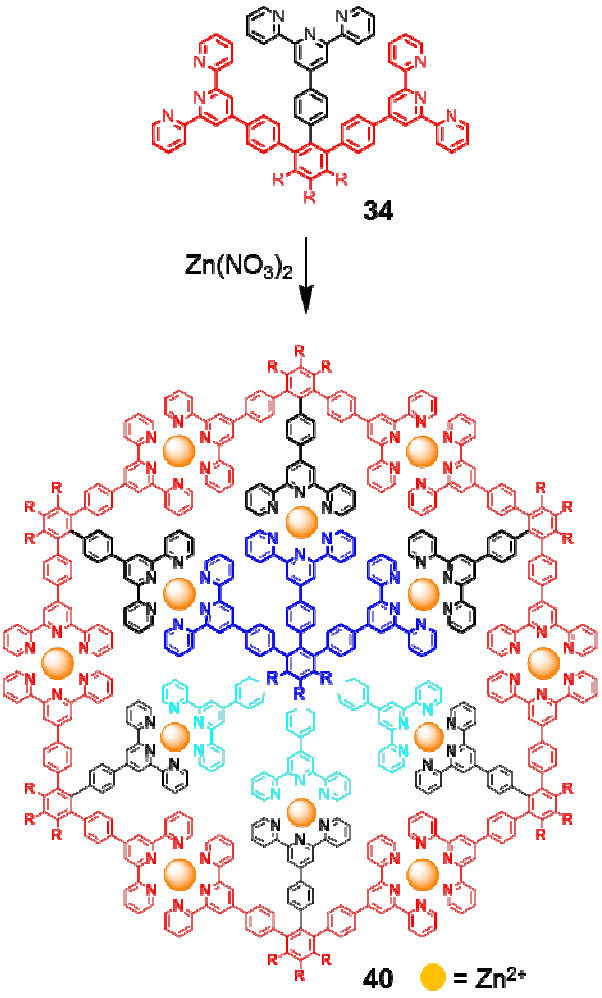

Scheme 14. Construction of a novel, highly distorted 3D molecular wheel **39**. The core terpyridines are shown as shades of blue for better visualization[68] [Redrawn with permission from Wiley-VCH, X. Lu, *et al.*, *Chem. J. Eur.*, 2014, DOI: 10.1002/chem.201404358].

From the above examples, it became apparent that an alternate approach would use vertices that are structurally predesigned to minimize the possible number of structural options and that the linear sides need to be used as the points of assembly. Thus, the final example in this tutorial will test the waters. The easy construction of the two "**V**" (**41**; for the vertices) and "**K**" (**42**, for the exterior walls) components of which each possessed the key markers (for testing the final symmetry) and rigidly directed terpyridines (for assembly of the sides of the triangles) followed known synthetic procedures from the corresponding polybromoarenes. To the dilute solution of a 1:1 ratio of ligands **41** and **42**, one simply adds 3 equivalents of

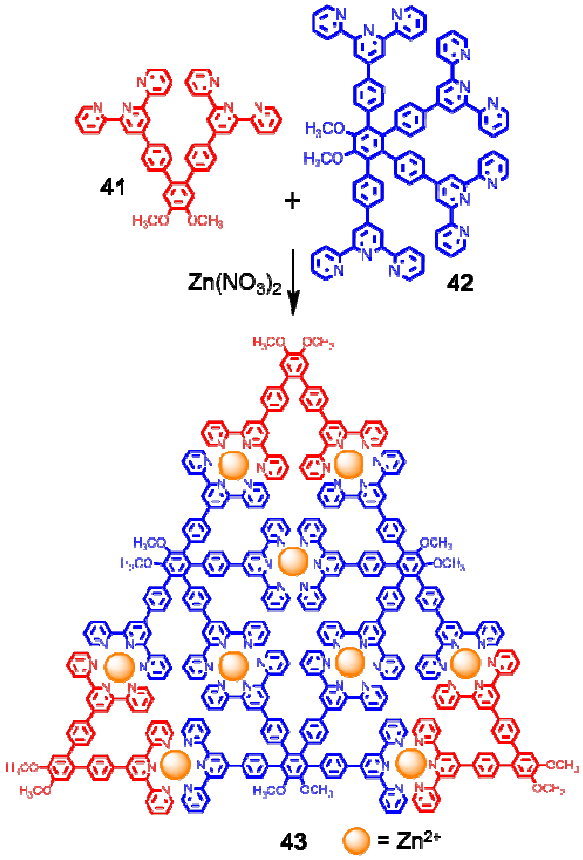

Scheme 15. The self-assembly of the G1 Sierpiński triangle **43**[76] [Redrawn with permission from Wiley-VCH, R. Sarkar, *et al.*, *Angew. Chem. Int. Ed.*, 2014, DOI: 10.1002/anie.201407285].

Cd^{2+} and the first generation Sierpiński triangle **43** self-assembled in near quantitative yield (Scheme 15).[76] The MS data demonstrated that there was a single product. The NMR also shows only two spikes at 3.98 (vertex) & 3.87 ppm (side wall) for the two different methoxy markers supporting a single highly symmetric product and under dilute conditions. The TEM images (Figure 14) also support the presence of a distinctive triangular structure possessing the correct dimensions. The TEM images also suggest that there can be aggregation at higher concentration which can be envisioned as by considering two triangles, one lying on top of another to generate the well-known Star of David; noteworthy at

higher concentrations, NMR data show a very slight shift for the side wall markers whereas the vertex markers are unaffected since they are all identical and in the same general environment.

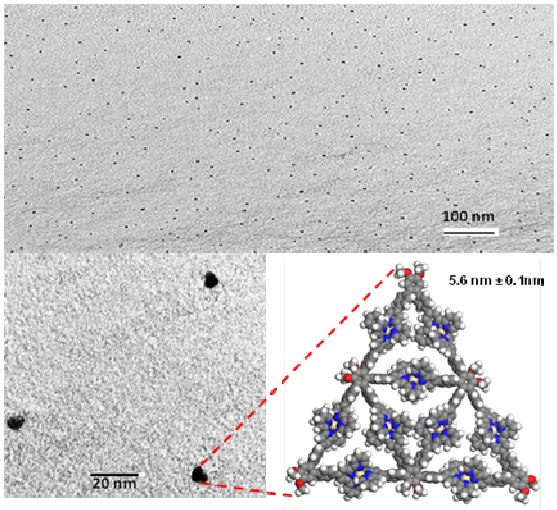

Figure 14. The TEM of the G1 Sierpiński triangle **43**[76] [Redrawn with permission from Wiley-VCH, R. Sarkar, *et al.*, *Angew. Chem. Int. Ed.*, 2014, DOI: 10.1002/anie.201407285].

"All our hopes for the future depend on a sound understanding of the past." Frederic Harrison (1831-1923) The transformation of Nature's chaos as seen through the lens of mathematics leading to the design and construction of novel fractal macromolecular assemblies that can possess utilitarian applications by the manipulation of their ordered placement of the metal centers is one of tomorrow's interesting challenges.

GRN would like to thank his numerous colleagues, who have assisted us and contributed to this growing fractal project over the years and are acknowledged on our publications. Support is also acknowledged from the National Science Foundation (DMR-08-12337, DMR-07-05015, CHE-11-51991) and The University of Akron.

Notes and references

[a]The Departments of Polymer Science and Chemistry, The University of Akron, Akron, OH 44325 USA. newkome@uakron.edu
[b]The Maurice Morton Institute for Polymer Science, The University of Akron, Akron, OH 44325 USA.

Reference List

1 P. B. Tomlinson, *Am. Sci.*, 1983, **71**, 141-149.

2 Forbes, P., *The Gecko's Foot: Bioinspiration - Engineered from Nature*, HarperCollins Publishers, London, 2005.

3 G. R. Newkome, Z. Yao, G. R. Baker, V. K. Gupta, *J. Org. Chem.*, 1985, **50**, 2003-2004.

4 T. J. Cho, C. N. Moorefield, P. Wang, G. R. Newkome, *ACS Symp. Ser.*, 2006, **921**, 186-204.

5 D. Farin, D. Avnir, *Angew. Chem. , Int. Ed. Engl.*, 1991, **30**, 1379-1380.

6 Mandelbrot, B. B., *Les Objets Fractals: Forme, Hasard et Dimension*, Flammarion, Paris, 1975.

7 Mandelbrot, B. B., *The Fractal Geometry of Nature*, Freeman, San Francisco, 1982.

8 W.-D. Jang, K. M. K. Selim, C.-H. Lee, I.-K. Kang, *Prog. Polym. Sci.*, 2009, **34**, 1-23.

9 G. R. Newkome, P. Wang, C. N. Moorefield, T. J. Cho, P. Mohapatra, S. Li, S.-H. Hwang, O. Lukoyanova, L. Echegoyen, J. A. Palagallo, V. Iancu, S.-W. Hla, *Science*, 2006, **312**, 1782-1785.

10 P. Wang, C. N. Moorefield, G. R. Newkome, *Angew. Chem. Int. Ed.*, 2005, **44**, 1679-1683.

11 Peitgen, H.-O., Jürgens, H., Saupe, D., *Chaos and Fractals. New Frontiers of Science*, Springer-Verlag, New York, 1992, 80.

12 Peitgen, H.-O., 'Personal assistance', 2011.

13 W. Sierpinski, *Comptes Rendus (Paris)*, 1915, **160**, 302-305.

14 B. Happ, A. Winter, M. D. Hager, U. S. Schubert, *Chem. Soc. Rev*, 2012, **41**, 2222-2255.

15 X. Chen, Y. Ding, Y. Cheng, L. Wang, *Synth. Met.*, 2010, **160**, 625-630.

16 A. C. Benniston, *Chem. Soc. Rev.*, 2004, **33**, 573-578.

17 Z. S. Yoon, Y.-T. Chan, S. Li, G. R. Newkome, T. G. Goodson, III, *J. Phys. Chem. B.*, 2010, **114**, 11731-11736.

18 S. Mignani, S. El Kazzouli, M. M. Bousmina, J.-P. Majoral, *Chem. Rev.*, 2014, **114**, 1327-1342.

19 G. R. Newkome, C. D. Shreiner, *Polymer*, 2008, **49**, 1-173.

20 G. R. Newkome, C. D. Shreiner, *Chem. Rev.*, 2010, **110**, 6338-6442.

21 A. Kumar, S. S. Sun, A. J. Lees, *Coord. Chem. Rev.*, 2008, **252**, 922-939.

22 C. Park, M. S. Im, S. Lee, J. Lim, C. Kim, *Angew. Chem. Int. Ed.*, 2009, **47**, 9922-9926.

23 B. W. Koo, C. K. Song, C. Kim, *Sens. Actuators, B*, 2001, **77**, 432-436.

24 E. Boisselier, L. Liang, M. Dalko-Csiba, J. Ruiz, D. Astruc, *Chem. Eur. J.*, 2010, **16**, 6056-6068.

25 C. Hartmann-Thompson, D. L. Keeley, J. R. Rousseau, P. R. Dvornic, *J. Polym. Sci. , Part A: Polym. Chem.*, 2009, **47**, 5101-5115.

26 *Dendrimer-Based Drug Delivery Systems From Theory to Practice*, John Wiley & Sons, Hoboken, N.J., 2012.

27 Bieniarz, C., *Encyclopedia of Pharmaceutical Technology*, Swarbrick, J., Boylan, J. C. eds., Marcel Dekker, Inc., New York, Volume 18, Supplement 1, 1999.

28 A. D'Emanuele, D. Attwood, *Adv. Drug Del. Rev.*, 2005, **57**, 2147-2162.

29 T. Darbre, J.-L. Reymond, *Acc. Chem. Res.*, 2006, **39**, 925-934.

30 P. Dhal, S. C. Polomoscanik, L. Z. Avila, S. R. Holmes-Farley, R. J. Miller, *Adv. Drug Del. Rev.*, 2009, **61**, 1121-1130.

31 C. Dufès, I. F. Uchegbu, A. G. Schätzlein, *Adv. Drug Delivery Rev.*, 2005, **57**, 2177-2202.

32 P. Govender, B. Therrien, *Eur. J. Inorg. Chem.*, 2012, 2853-2862.

33 S. Mignani, S. El Kazzouli, M. Bousmina, J.-P. Majoral, *Adv. Drug Del. Rev.*, 2013, **65**, 1316-1330.

34 J. B. Wolinsky, M. W. Grinstaff, *Adv. Drug Del. Rev.*, 2008, **60**, 1037-1055.

35 D. Astruc, *J. Organomet. Chem.*, 2011, **696**, 2864-2869.

36 L. Xu, L.-J. Chen, H.-B. Yang, *Chem. Commun.*, 2014, **50**, 5156-5170.

37 A.-M. Caminade, R. Laurent, A. Ouali, *Inorg. Chim. Acta*, 2014, **409**, 68-88.

38 G. R. Newkome, T. J. Cho, C. N. Moorefield, G. R. Baker, M. J. Saunders, R. Cush, P. S. Russo, *Angew. Chem. Int. Ed.*, 1999, **38**, 3717-3721.

39 G. R. Newkome, J. K. Young, G. R. Baker, R. L. Potter, L. Audoly, D. Cooper, C. D. Weis, K. F. Morris, C. S. Johnson, Jr., *Macromolecules*, 1993, **26**, 2394-2396.

40 P. Wang, C. N. Moorefield, K.-U. Jeong, S.-H. Hwang, S. Li, S. Z. D. Cheng, G. R. Newkome, *Adv. Mater.*, 2008, **20**, 1381-1385.

41 J. K. Young, G. R. Baker, G. R. Newkome, K. F. Morris, C. S. Johnson, Jr., *Macromolecules*, 1994, **27**, 3464-3471.

42 C. Friebe, M. D. Hager, A. Winter, U. S. Schubert, *Adv. Mater.*, 2012, **24**, 332-345.

43 C. Friebe, A. Wild, J. Perelaer, U. S. Schubert, *Macromol. Rapid Commun.*, 2012, **33**, 503-509.

44 A. Winter, S. Hoeppener, G. R. Newkome, U. S. Schubert, *Adv. Mater.*, 2011, **23**, 3484-3498.

45 A. Winter, G. R. Newkome, U. S. Schubert, *ChemCatChem*, 2011, **3**, 1384-1406.

46 A. Winter, M. D. Hager, G. R. Newkome, U. S. Schubert, *Adv. Mater.*, 2011, **23**, 5728-5748.

47 S.-H. Hwang, C. N. Moorefield, F. R. Fronczek, O. Lukoyanova, L. Echegoyen, G. R. Newkome, *Chem. Commun.*, 2005, 713-715.

48 X. Lu, X. Li, J.-L. Wang, C. N. Moorefield, C. Wesdemiotis, G. R. Newkome, *Chem. Commun.*, 2012, **48**, 9873-9875.

49 N. Miyaura, A. Suzuki, *Chem. Rev.*, 1995, **95**, 2457-2483.

50 T. Schröder, R. Brodbeck, M. C. Letzel, A. Mix, B. Shnatwinkel, M. Tonigold, D. Volkmer, J. Mattay, *Tetrahedron Lett.*, 2009, **49**, 5939-5942.

51 A. Schultz, Y. Cao, M. Huang, S. Z. D. Cheng, X. Li, C. N. Moorefield, C. Wesdemiotis, G. R. Newkome, *Dalton Trans.*, 2012, **41**, 11573-11575.

52 K. Kokado, Y. Chujo, *Dalton Trans.*, 2011, **40**, 1919-1923.

53 J. M. Ludlow III, M. Tominaga, Y. Chujo, A. Schultz, X. Lu, T. Xie, K. Guo, C. N. Moorefield, C. Wesdemiotis, G. R. Newkome, *Dalton Trans.*, 2014, **43**, 9604-9611.

54 Dobrawa, R., Ballester, P., Saha-Möller, C. R., Würthner, F., *Metal-Containing and Metallosupramolecular Polymers and Materials*, Schubert, U. S., Newkome, G. R., Manners, I. eds., ACS Symposium Series, Washington, D.C., 2006.

55 F. Caruso, C. Schüler, D. G. Kurth, *Chem. Mater.*, 1999, **11**, 3394-3399.

56 P. Lehmann, D. G. Kurth, G. Brezesinski, C. Symietz, *Chem. Eur. J.*, 2001, **7**, 1646-1651.

57 A. Schultz, X. Li, J. K. McCusker, C. N. Moorefield, F. N. Castellano, C. Wesdemiotis, G. R. Newkome, *Chem. Eur. J.*, 2012, **18**, 11569-11572.

58 I. P. Evans, E. A. Spencer, G. Wilkinson, *J. Chem. Soc., Dalton Trans.*, 1973, 204-209.

59 Y.-T. Chan, X. Li, C. N. Moorefield, C. Wesdemiotis, G. R. Newkome, *Chem. Eur. J.*, 2011, **17**, 7750-7754.

60 Y.-T. Chan, X. Li, J. Yu, G. A. Carri, C. N. Moorefield, C. Wesdemiotis, G. R. Newkome, *J. Am. Chem. Soc.*, 2011, **133**, 11967-11976.

61 S.-H. Hwang, P. Wang, C. N. Moorefield, L. A. Godínez, J. Manríquez, E. Bustos, G. R. Newkome, *Chem. Commun.*, 2005, 4672-4674.

62 Y.-T. Chan, C. N. Moorefield, M. Soler, G. R. Newkome, *Chem. Eur. J.*, 2010, **16**, 1768-1771.

63 Y.-T. Chan, X. Li, M. Soler, J.-L. Wang, C. Wesdemiotis, G. R. Newkome, *J. Am. Chem. Soc.*, 2009, **131**, 16395-16397.

64 A. Schultz, X. Li, B. Barkakaty, C. N. Moorefield, C. Wesdemiotis, G. R. Newkome, *J. Am. Chem. Soc.*, 2012, **134**, 7672-7675.

65 J.-L. Wang, X. Li, X. Lu, I.-F. Hsieh, Y. Cao, C. N. Moorefield, C. Wesdemiotis, S. Z. D. Cheng, G. R. Newkome, *J. Am. Chem. Soc.*, 2011, **133**, 11450-11453.

66 T. Bauer, A. D. Schlüter, J. Sakamoto, *Synlett*, 2010, 877-880.

67 X. Lu, X. Li, Y. Cao, A. Schultz, J.-L. Wang, C. N. Moorefield, C. Wesdemiotis, S. Z. D. Cheng, G. R. Newkome, *Angew. Chem. Int. Ed.*, 2013, **52**, 7728-7731.

68 X. Lu, X. Li, K. Guo, J. Wang, M. Huang, J.-L. Wang, T.-Z. Xie, C. N. Moorefield, S. Z. D. Cheng, C. Wesdemiotis, G. R. Newkome, *Chem. Eur. J.*, 2014, DOI: 10.1002/chem.201404358

69 K. Fujibashi, R. Hariadi, S. H. Park, E. Winfree, S. Murata, *Nano Lett.*, 2014, **8**, 1791-1797.

70 D. Nieckarz, P. Szabelski, *J. Phys. Chem. C*, 2014, **117**, 11229-11241.

71 D. Nieckarz, P. Szabelski, *Chem. Commun.*, 2014, **50**, 6843-6845.

72 F. Würthner, C.-C. You, C. R. Saha-Möller, *Chem. Soc. Rev.*, 2004, **33**, 133-146.

73 R. Chakrabarty, P. S. Mukherjee, P. J. Stang, *Chem. Rev.*, 2011, **111**, 6810-6918.

74 T. R. Cook, Y.-R. Zheng, P. J. Stang, *Chem. Rev.*, 2013, **113**, 734-777.

75 B. H. Northrop, Y. R. Zheng, K. W. Chi, P. J. Stang, *Acc. Chem. Res.*, 2009, **42**, 1554-1563.

76 R. Sarkar, K. Guo, C. N. Moorefield, M. J. Saunders, C. Wesdemiotis, G. R. Newkome, *Angew. Chem. Int. Ed.*, 2014, DOI: 10.1002/anie.201407285

